Mon. Not. R. Astron. Soc. **329,** 747–758 (2002)

The distribution of atomic gas and dust in nearby galaxies – I. Presentation of matched-resolution VLA H I and SCUBA 850-μm maps

H. C. Thomas,[1★] L. Dunne,[2] M. S. Clemens,[1] P. Alexander,[1] S. Eales[2] and D. A. Green[1]
[1]*Cavendish Laboratory, Madingley Road, Cambridge CB3 0HE*
[2]*Department of Physics and Astronomy, University of Wales Cardiff, PO Box 913, Cardiff CF2 3YB*

Accepted 2001 September 14. Received 2001 September 6; in original form 2001 June 28

ABSTRACT

We present matched-resolution VLA H I and SCUBA 850-μm maps of 20 *IRAS*-bright galaxies. Of the galaxies observed, two were not detected in H I and two were detected in absorption. The H I distributions of the galaxies have a range of morphologies. Some of the systems appear H I deficient in the central regions which could be due to a high conversion rate of H I into molecules or H I absorption. In contrast to the H I, the 850-μm emission has a smooth distribution which is concentrated towards the optical centre of each galaxy. We also find evidence for 850-μm emission extending to the periphery of the optical disc in some of the galaxies. Finally, we note that the relative lack of 850-μm emission when compared with H I does not necessarily mean that the atomic gas and dust do not have similar mass distributions.

Key words: galaxies: ISM – radio lines: galaxies – submillimetre.

1 INTRODUCTION

Despite considerable observational effort during the past 5 years, the distribution of dust mass within galaxies remains very poorly constrained relative to the molecular and atomic gas [for reviews of molecular and atomic gas in galaxies, see Young & Scoville (1991) and Giovanelli & Haynes (1988) respectively]. Knowledge about the distribution of dust *mass* (rather than infrared emission) is crucial to our understanding of galaxy evolution, for many reasons.

(i) The extinction at any given point in a galaxy is a strong function of the distribution of dust. Dust could be very clumped, leading to an optical depth $\tau \ll 1$ throughout most of the disc with regions of $\tau \gg 1$ having a very low filling factor. Alternatively, a rather smooth dust distribution would lead to an intermediate optical depth throughout the entire disc. The true situation undoubtedly lies between these extremes. The difference between these scenarios is crucial to the interpretation of observations at any wavelength that suffers from extinction by dust (e.g. optical, ultraviolet).

(ii) Dust is generally considered to be the site of formation of molecules in the interstellar medium (ISM); see Whittet (1992) for a detailed discussion. An understanding of how the ISM is processed through the atomic, molecular and ionized phases thus requires knowledge of how the dust is distributed. Is dust sufficiently long-lived that it can move from one phase of the ISM to another? If a significant mass of dust is associated with the atomic gas in galactic discs then how did it get there, and how long can it survive without being replenished? The dust mass associated with molecular and atomic phases of the ISM at a given time is an important constraint on these questions.

(iii) Is the metallicity gradient observed in disc galaxies associated with a similar gradient in the dust mass? Differences in the rate of fall-off of dust mass and metallicity will constrain the processes involved in converting metals to grains, and vice versa.

(iv) The extent of the dust distribution in disc galaxies is not known. Evidence has been found that the dust distribution extends significantly beyond the optical disc (Davies et al. 1999; Trewhella et al. 2000). If dust does extend out to large radii, then there may be extinction towards background sources (e.g. high-redshift supernovae: Alton et al. 2001).

A small number of nearby galaxies have been studied in detail using the Submillimetre Common User Bolometer Array (SCUBA): e.g. NGC 891 (Alton et al. 1998, 2000), NGC 7331 (Bianchi et al. 1998; Alton et al. 2001), NGC 4038/9 (Haas et al. 2000) and NGC 6946 (Bianchi et al. 2000). In all cases a good correlation has been found between the distribution of molecular gas and the 850-μm emission, providing strong evidence that molecular gas and dust are closely associated. Although the dust associated with molecular clouds dominates the 850-μm emission, it does not necessarily imply that most of the dust mass in galaxies is associated with the molecular ISM. Recent observations of our Galaxy have revealed a strong correlation between H I column density and a cool dust component (Boulanger et al. 1996). However, comparison of the submillimetre and H I emission at the periphery of a few nearby galaxies has shown that they are not always correlated (e.g. NGC 7331: Alton et al. 2001).

★E-mail: hct24@mrao.cam.ac.uk

The determination of the dust mass distribution is complicated because the far-infrared emission that is used as a tracer of dust depends not only on the dust mass but also on the dust temperature and the grain properties. The emission from galaxies at short far-infrared wavelengths ($<100\mu$m) is dominated by warm dust, but this may not necessarily contain the bulk of the dust mass. The scale of the problem is reduced by observing at long infrared wavelengths where approximate Rayleigh–Jeans conditions are met (emission $\propto T$). The long-wavelength filters and the spatial resolution (15 arcsec at 850 μm) make SCUBA a very good instrument with which to determine the distribution of cool dust in nearby galaxies.

In this paper we present Very Large Array (VLA) H I snapshot observations of 20 *IRAS*-bright galaxies which have been selected in order to compare with SCUBA 850-μm data. This is the first survey of a large sample of galaxies in which the resolution of the H I observations is comparable to that of the 850-μm observations. A detailed analysis of the gas and dust mass distributions will be presented in a future paper. Here, we present the 850-μm and H I maps, comment on some of the individual galaxies and discuss general trends.

2 SCUBA DATA

The galaxies that we observed at 21 cm were selected from the *IRAS*-bright SCUBA Local Universe Galaxy Survey (SLUGS: Dunne et al. 2000). SLUGS consists of 104 galaxies with declination in the range $-10°$ to $50°$ and velocity $>1900\,\mathrm{km\,s^{-1}}$. Each galaxy in the survey was observed at 850 μm in 'jiggle map' mode using the SCUBA instrument on the James Clerk Maxwell Telescope (JCMT). The total integration time on each object was typically 15 min. Further details regarding the observations and data reduction are described by Dunne et al. (2000). The unsmoothed maps have a field of view of 2.3 arcmin, a resolution of 15 arcsec and an rms noise of $\sim$10 mJy beam^{-1}.

3 VLA DATA

3.1 Observations and data reduction

The primary objective of this study is to compare the H I and 850-μm emission at the periphery of the optical disc (the R_{25} radius). Galaxies were selected from the SLUGS sample with angular sizes (R_{25}) less than 3 arcmin. From this we chose 20 galaxies to observe at 21 cm, based on the LST ranges allocated for the VLA observations. The sample included NGC 3110, a galaxy with no previously reported H I measurements in the literature. Only one of the galaxies in the sample has published interferometric H I maps (NGC 7714). Table 1 lists the sample.

The 21-cm snapshot observations were made in 2000 May using the C-array configuration of the VLA. Observations were made using the 1A correlator mode giving 64 channels with on-line Hanning smoothing and a bandwidth of 6.25 MHz, resulting in a channel width of 21 km s^{-1}. Owing to the large range of recession velocities of the galaxies in the sample (2050–11 782 km s^{-1}), the frequency setting of the central channel varied. To maximize the time spent on-source, galaxies with similar recession velocities and linewidths were observed at the same frequency setting. The primary calibrator was either 0134+329 (flux density = 16.10 Jy) or 1328+307 (flux density = 14.89 Jy), and these were observed at each frequency setting. Phase calibrators were observed for 2 min before and after each source. The total integration time per galaxy was typically 15 min.

The data were reduced using the Astronomical Image Processing System (AIPS) package. After removing bad data and calibration, 'dirty' line cubes were produced and the channels were inspected for line emission. In the majority of cases, the 1.4-GHz continuum

Table 1.

Name	RA (B1950)	Dec. (B1950)	Morph. type	Spec. type	Distance $75/H_0$ (Mpc)	$\log_{10}(L_{\rm fir})$ $L_\odot$	Notes
(1)	(2)	(3)	(4)	(5)	(6)	(7)	(8)
NGC 2785	09 12 03.4	+41 07 33	Im?	H II	36.5	10.42	
UGC 4881^p	09 12 39.6	+44 32 20	S?	H II	157.1	11.50	
NGC 2856	09 20 53.2	+49 27 49	S?		35.2	10.18	
NGC 2990	09 43 40.1	+05 56 23	Sc:		41.1	10.30	
UGC 5376	09 57 51.3	+03 36 54	Sdm:		27.3	10.00	
NGC 3110	10 01 32.1	−06 13 58	SB(rs)b pec	H II	67.1	11.06	
NGC 3221	10 19 35.5	+21 49 19	SB(s)cd: sp		54.8	10.79	
NGC 3583	11 11 22.3	+48 35 33	SB(s)b		28.7	10.22	
NGC 3994/5	11 55 06.0	+32 33 51	SA(rs)c/SAm pec	Sbrst/H II	41.8	10.53	*
NGC 4418	12 24 20.3	−00 36 09	(R′)SAB(s)a	Sey1; Sey2	29.1	10.68	*
NGC 5104	13 18 49.4	+00 36 17	Sa:	LINER	74.4	10.90	
UGC 8739	13 47 02.0	+35 30 17	SB?		67.1	10.84	
NGC 5433	14 00 24.0	+32 44 58	Sdm:		58.1	10.65	
NGC 5600	14 21 26.1	+14 51 51	Sc pec		30.9	10.09	
NGC 5665	14 29 57.6	+08 18 05	SAB(rs)c pec?	LINER; H II	29.7	10.07	*
NGC 5900	15 13 16.4	+42 23 41	Sb: sp		33.5	10.32	
NGC 5929/30	15 24 19.8	+41 50 48	Sab:/SAB(rs)b	Sey2/H II	34.0	10.34	*
NGC 5936	15 27 39.7	+13 09 40	SB(rs)b	H II	53.4	10.73	
NGC 6052^p	16 03 01.3	+20 40 43	S?	Sbrst	62.9	10.69	
NGC 7714	23 33 41.2	+01 52 42	SB(s)b: pec	H II; LINER	37.3	11.14	*

(1) Galaxy name. A '^{p}' denotes those galaxies that consist of a pair. (2)–(3) RA and Dec. (B1950) taken from NED. (4) Morphological type taken from NED. (5) Spectral type taken from NED, except for NGC 5665 (taken from Artamonov et al. 2000), NGC 6052 (taken from Condon, Frayer & Broderick 1991) and NGC 4418 (taken from Kawara et al. 1990). (6) Distance, calculated from the recession velocity given in NED. (7) Far-infrared luminosity from Dunne et al. (2000). (8) See notes on individual galaxies for those indicated by a '*'.

Table 2. Gas and dust masses.

Name	$S_{\rm HI} \pm \sigma$ (Jy km s^{-1})	$\log_{10}(M_{\rm HI})$ ($M_\odot$)	$\log_{10}(M_{\rm d})$ ($M_\odot$)	$\log_{10}(M_{\rm H_2})$ ($M_\odot$)	$\frac{M_{\rm H_2}}{M_{\rm HI}}$	$\frac{M_{\rm HI}+M_{\rm H_2}}{M_{\rm d}}$
(1)	(2)	(3)	(4)	(5)	(6)	(7)
NGC 2785	1.79 ± 0.53	8.75	7.20	–	–	–
UGC 4881^p	<1.53	<9.95	7.94	–	–	–
NGC 2856	<2.52	<8.87	6.80	9.62^a	>5.60	<778
NGC 2990	10.94 ± 0.99	9.64	7.05	–	–	–
UGC 5376	10.18 ± 0.94	9.25	6.83	–	–	–
NGC 3110	2.89 ± 0.85	9.49	7.73	10.34^b	7.10	465
NGC 3221	22.16 ± 1.52	10.20	7.73	9.95^b	0.60	461
NGC 3583	11.97 ± 0.77	9.36	7.06	9.50^b	1.40	102
NGC 3994/5	11.43 ± 0.77	9.67	7.41	9.41^a	0.50	282
NGC 4418	A	–	6.86	9.18^b	–	–
NGC 5104	3.35 ± 1.32	9.64	7.51	–	–	–
UGC 8739	6.91 ± 0.5	9.87	7.75	–	–	–
NGC 5433	3.32 ± 0.75	9.42	7.49	–	–	–
NGC 5600	3.81 ± 0.51	8.93	6.89	8.96^c	1.10	227
NGC 5665	3.07 ± 0.59	8.81	7.20	9.05^c	1.70	112
NGC 5900	7.53 ± 0.93	9.30	7.14	...	–	–
NGC 5929/30	A	–	6.92	9.06^d	–	–
NGC 5936	2.67 ± 0.48	9.25	7.43	9.79^b	3.50	295
NGC 6052^p	6.09 ± 0.88	9.75	7.32	10.23^a	3.00	1082
NGC 7714	7.32 ± 0.75	9.38	6.68	9.47^b	1.20	1118
Milky Way	–	9.54	–	9.13	0.40	–

(1) Galaxy name. A '^{p}' denotes those galaxies that consist of a pair. The molecular and atomic gas masses for the Milky Way taken from Sodroski et al. (1997) are included for comparison. (2) VLA H I flux and error. Galaxies indicated with an 'A' were only detected in absorption. (3) The mass of H I calculated from $2.36 \times 10^5 D^2 S_{\rm HI}$, where D is the distance to the source (in Mpc). (4) Dust mass taken from Dunne et al. (2000). (5) Molecular gas mass, assuming a CO-to-H_2 conversion factor of $X = 2.8 \times 10^{20}$ H_2 cm^{-2} (Kenney & Young 1989). The CO fluxes are from the following papers: ^{a} Sofue et al. (1993); ^{b} Sanders, Scoville & Soifer (1991); ^{c} Casoli et al. (1996); ^{d} Maiolino et al. (1997). (6) Molecular gas to atomic gas mass ratio calculated from columns (3) and (5). (7) Gas-to-dust mass ratio calculated from columns (3)–(5).

source dominated over the line emission, so spectra were made from the dirty line maps in order to identify the line emission. After the channels containing line emission were identified, the continuum component was subtracted in the u–v plane by fitting a straight line to the line-free channels. Naturally weighted maps were then made and CLEANed. After primary beam correction the rms noise per channel, $\sigma_{\rm rms}$, in the CLEANed maps was typically 1–2 mJy beam^{-1}.

Integrated intensity (moment 0) maps were made by summing the channels containing line emission using a combination of the 'cut-off' and 'window' methods (van Gorkom & Ekers 1988). Each data cube was smoothed over 3 (velocity) channels and 5 pixels using a boxcar function. If the resulting pixel value after smoothing was greater than $1.5\sigma_{\rm rms}$ (the 'cut-off') then it was included in the sum. This was an effective way of identifying diffuse extended H I emission.

The synthesized beam varied from 15 to 25 arcsec (FWHM). For a channel width of 21 km s^{-1}, this corresponds to an H I column density detection limit of $\sim 2 \times 10^{20}$ atom cm^{-2}. In snapshot mode, the largest structures that can be mapped are ~3 arcmin; roughly half that attainable from a full synthesis observation at the zenith.

In order to compare the distributions of H I and 850-μm emission, the 850-μm and H I maps were convolved to the same resolution (25 arcsec). Each map was re-gridded so that it could be overlaid on an optical (R-band) map taken from the Digitized Sky Survey with a pixel size of 1.7 arcsec.

3.2 Flux measurements and errors

Of the 20 galaxies observed in H I, two were not detected (UGC 4881 and NGC 2856), and two were detected in absorption (NGC 4418 and NGC 5929). The total H I flux density of each galaxy was measured from the integrated H I map. We have not attempted to estimate the H I flux for galaxies detected in absorption. The error on each flux measurement was estimated from $\sigma_{\rm rms}\Delta V_{\rm ch}\sqrt{N_{\rm ch}}$, where $\sigma_{\rm rms}$, the rms noise, is measured over an area in one channel equivalent to the area of emission on the integrated map, $N_{\rm ch}$ is the number of channels containing emission and $\Delta V_{\rm ch}$ is the channel width (= 21 km s^{-1}). For galaxies not detected, we derived a $3\sigma_{\rm rms}$ upper limit for the amount of H I by assuming a typical velocity width of 350 km s^{-1}. In this case, the rms noise was calculated by

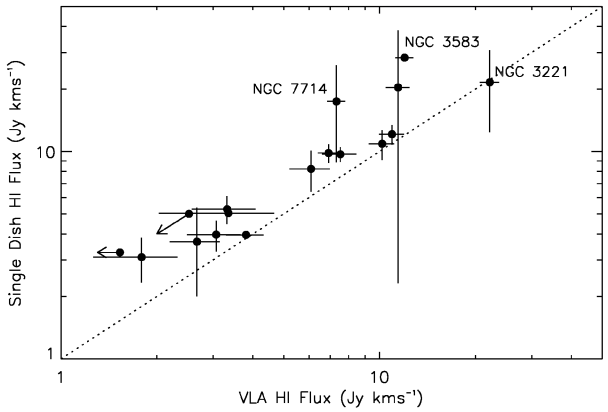

Figure 1. The mean single-dish H I fluxes from NED versus the VLA H I fluxes from this survey. The dotted line is the line of equality. See the text for discussion about NGC 3221, 3583 and 7714.

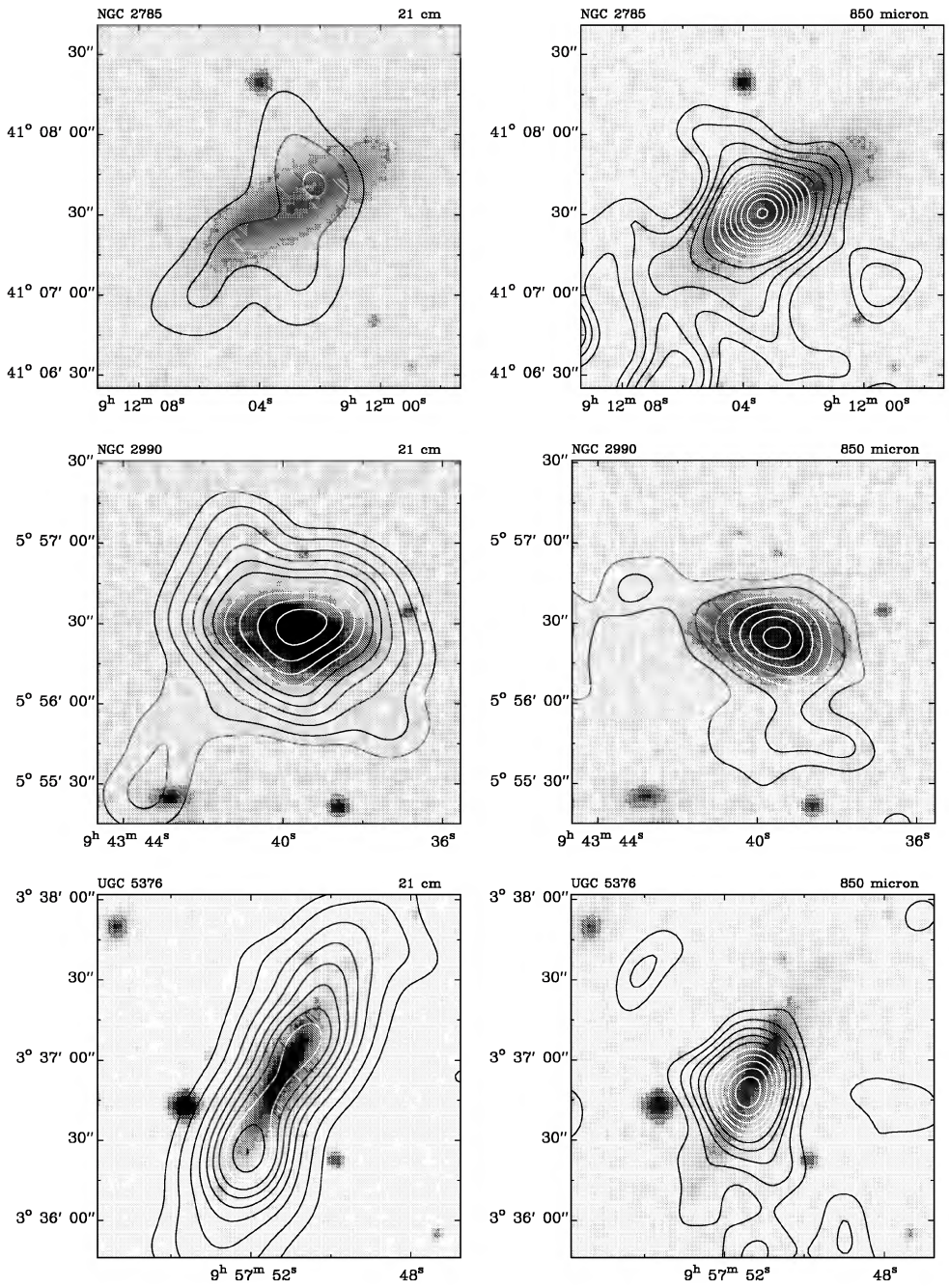

Figure 2. VLA C-array H I maps (left) and SCUBA 850-μm maps (right) convolved to a resolution of 25 arcsec and overlaid on an optical (*R*-band) Digitized Sky Survey image. The contours for the H I maps are $\pm 0.2, \pm 0.5, \pm 1.0, \pm 1.5, \pm 2.0 \ldots \times 10^{21}$ atom cm^{-2} where the dashed contours are negative and the solid contours are positive. The contours for the 850-μm maps are 10, 20, 30, 40 ... mJy beam^{-1} except for NGC 4418 which has contours at 10, 20, 40, 60 ... mJy beam^{-1}. The maps are all 2.3 arcmin^2 (the same as the SCUBA field of view), except NGC 3994/5 which consists of two SCUBA fields mosaicked together (~4 arcmin^2).

assuming that the H I was smoothly distributed over the same area as the continuum source in each velocity channel. All the fluxes and errors are quoted in Table 2. The errors do not include the calibration error which is estimated to be 5–10 per cent.

3.3 Comparison with single-dish measurements

In Fig. 1 we compare our derived H I fluxes with single-dish values taken from the NASA/IPAC Extragalactic Database (NED). If more than one single-dish H I measurement exists in the data base then the mean value is plotted and the error bars indicate the range of values. The error in calculating the VLA H I flux is also shown. The arrows give upper limits to the VLA H I flux for those galaxies not detected.

In general, 50–100 per cent of the H I flux compared with single-dish measurements is recovered in the VLA data. The largest discrepancies between single-dish and VLA H I fluxes are found for NGC 3583 and NGC 7714. Published VLA B-, C- and

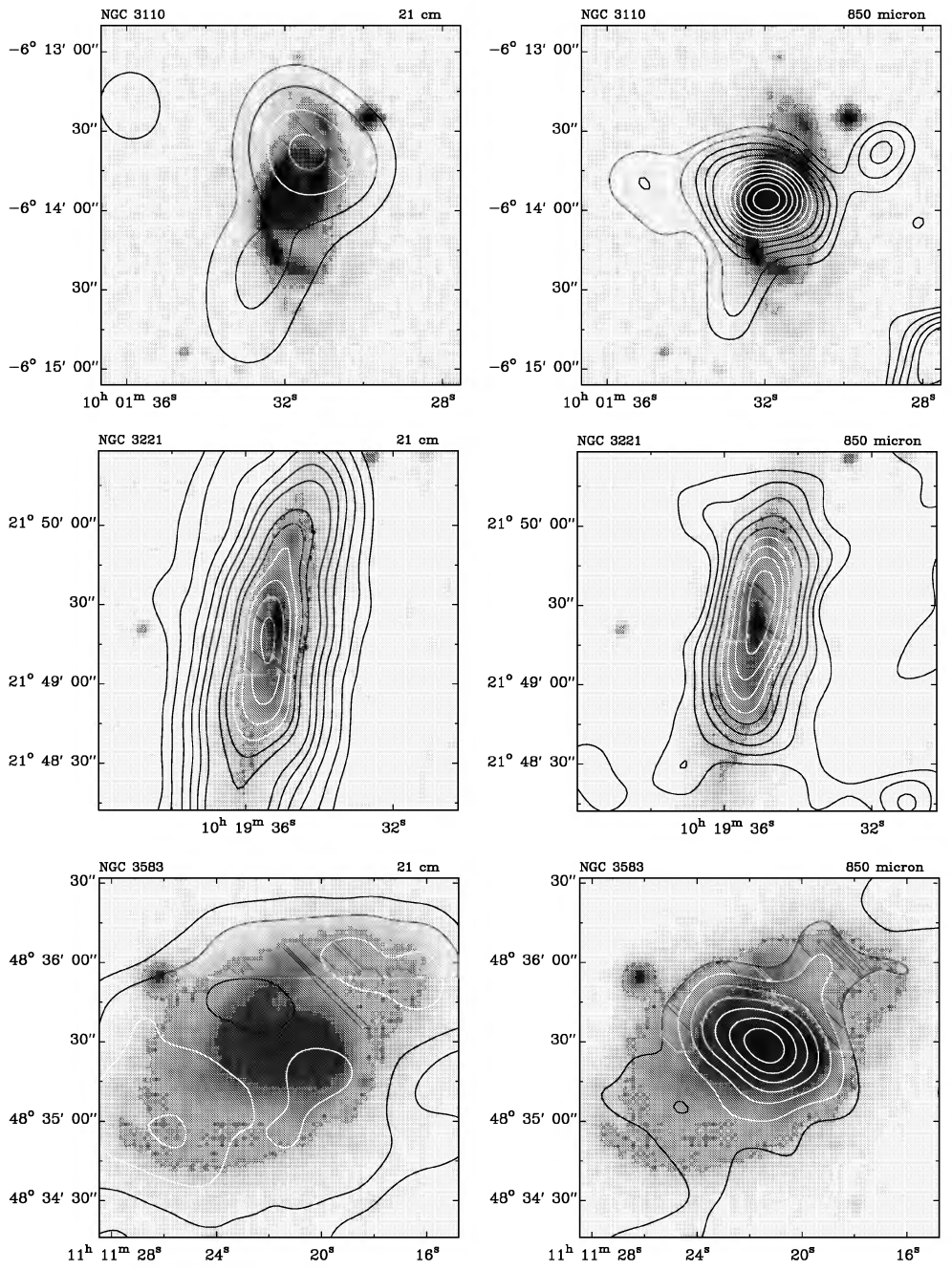

Figure 2 – *continued*

D-array maps of NGC 7714 show bridges of atomic gas connecting the galaxy with NGC 7715 (Smith & Wallin 1992; Smith, Struck & Pogge 1997). The gas in this system is very extended (~5 arcmin) and of low column density (~10^{18} cm^{-2}) which could not be detected by our short observations. Similarly, the atomic gas associated with NGC 3583 was not detected because of its large extent (NGC 3583 has the largest angular size of the galaxies in the sample with $R_{25} \sim 3$ arcmin) and low column density. The closest agreement between single-dish and VLA H I fluxes was found for highly inclined non-interacting galaxies with a correspondingly high column density, e.g. NGC 3221.

Given that the H I fluxes are in reasonable agreement with single-dish values, we are satisfied that the maps represent the true distribution of H I, and may be compared with the SCUBA 850-μm maps. The maps are shown in Figs 2 and 3. It is worth noting that both the H I and 850-μm observations are not sensitive to structures on scales greater than 3 and 2 arcmin respectively.

4 NOTES ON INDIVIDUAL GALAXIES

In this section we comment on some of the galaxies in the sample and compare the H I and 850-μm observations with other data, taken from the literature. These galaxies are indicated with a '*' in Table 1.

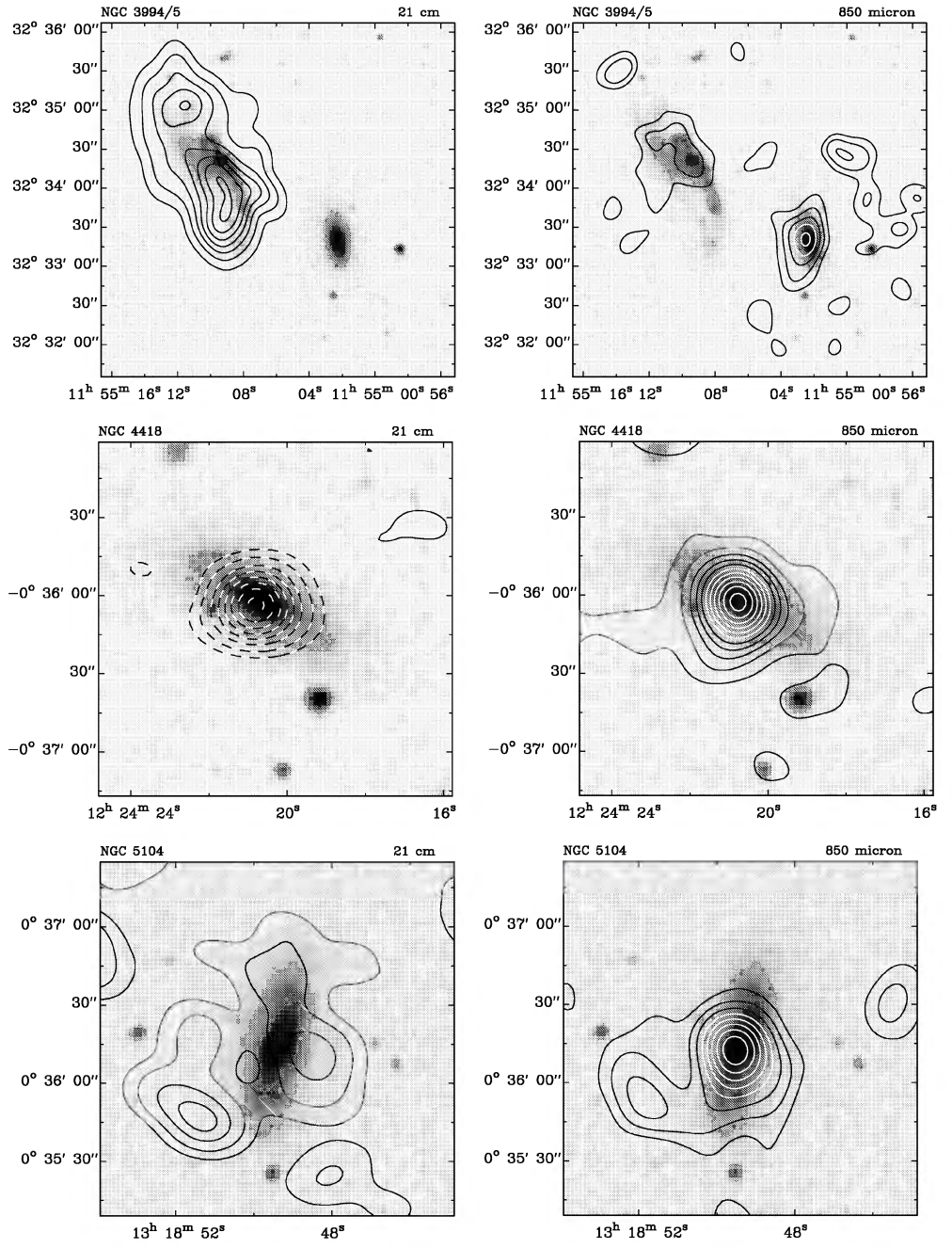

Figure 2 – *continued*

4.1 NGC 3994/5

NGC 3994 and 3995 are seperated by ~1.8 arcmin and are interacting with the galaxy NGC 3991 which lies 3.7 arcmin to the north-west of the pair. The triplet are also known as Arp 313 (Arp 1966). Baldwin, Phillips & Terlevich (1981) classified NGC 3994 as a LINER. A red continuum map shows that NGC 3994 has a complex structure with vigourous star formation in the outer ring-like arms and in wisps extending out of the galaxy (Keel et al. 1985). NGC 3995 also shows signs of active star formation, with ~20 high-luminosity H II regions apparent in an Hα map of the galaxy (Keel et al. 1985). Both NGC 3995 and NGC 3994 were only weakly detected at 850 μm. Single-dish H I observations have measured fluxes ranging from 10.32 to 46.4 Jy km s^{-1}. All of these observations suffered from varying degrees of confusion with nearby sources, depending on the pointing centre and size of the beam. We have measured a flux of 11.43 Jy km s^{-1} from NGC 3995, but do not detect any emission from NGC 3994.

4.2 NGC 4418

NGC 4418 is thought to contain a heavily enshrouded nucleus in the early stages of active galactic nucleus (AGN) activity (Roche et al. 1986; Roche & Chandler 1993; Spoon et al. 2001). In the radio, 95 per cent of the total 1.4-GHz flux comes from the central 0.5-arcsec region of the galaxy (Condon 1990; Kawara et al. 1990).

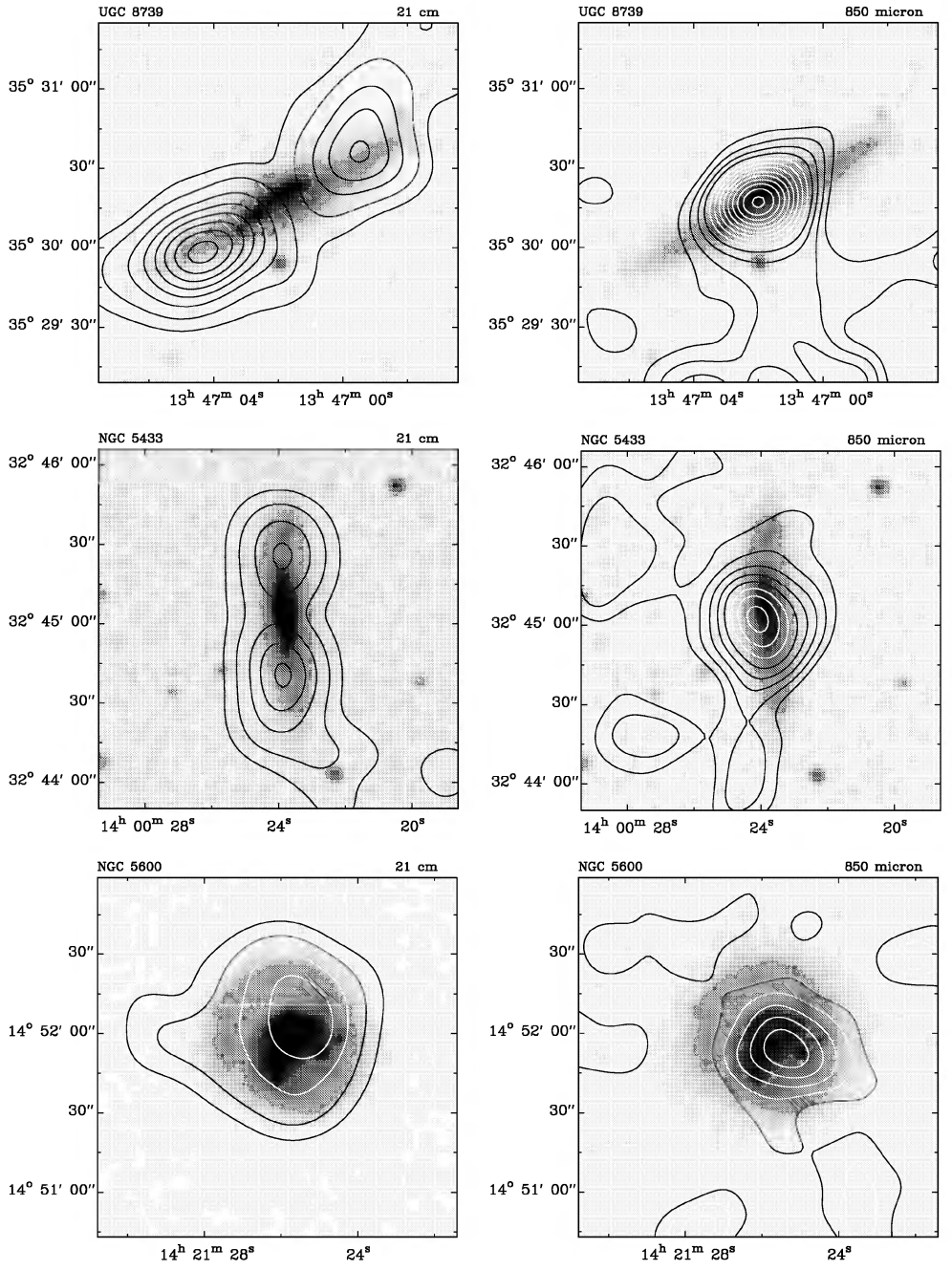

Figure 2 – *continued*

From ^{12}CO ($J = 1 \rightarrow 0$) observations, a molecular gas mass of 4×10^8 M$_\odot$ is inferred in the central 15-arcsec region of the galaxy (Kawara et al. 1990). Kawara et al. (1990) hypothesize that radiation from the nucleus is absorbed by dense ambient gas which then re-emits in the far-infrared. This is consistent with the strong 850-μm emission (it is the most luminous galaxy in the sample) and H I absorption concentrated towards the centre of the galaxy. We do not detect any H I emission. There is only one other H I observation of NGC 4418 in the literature. Richter & Huchtmeier (1987) measured an H I flux of 2.78 ± 0.46 Jy km s^{-1} using the Greenbank 300-foot telescope (HPBW $\sim$ 9 arcmin). However, we suspect that this emission is confused with the galaxy VV655, $\sim$3 arcmin away from NGC 4418 with a similar recession velocity. We detected VV655 in H I with a flux of 2.0 ± 0.7 Jy km s^{-1}.

4.3 NGC 5665 (Arp 49)

Although NGC 5665 has a somewhat asymmetric optical morphology, the peak in the 850-μm emission does agree with the peak in the *R*-band optical image, which is also the radio centre (see Condon 1990). Artamonov, Badan & Gusev (2000) examined the stellar populations of NGC 5665 using *BVRI* photometry. They suggested that NGC 5665 merged with a small companion galaxy 5×10^8 yr ago, causing a burst of star formation which was

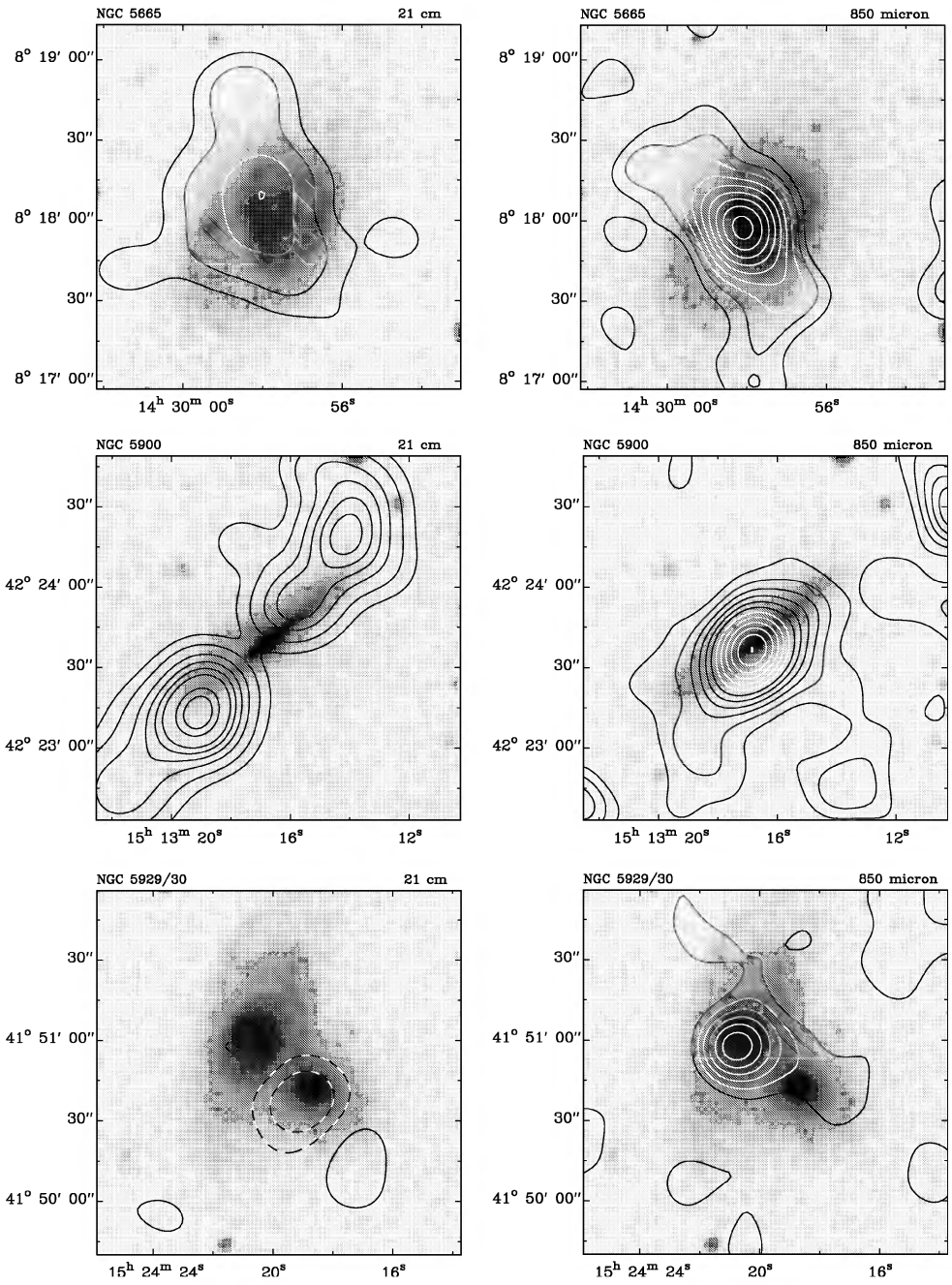

Figure 2 – *continued*

strongest in the south-eastern part of the disc. This corresponds to the peak in the 850-μm emission. Suprisingly, the H I emission (although having a somewhat irregular distribution) is not significantly offset from the optical centre of the galaxy.

4.4 NGC 5929/30 (Arp 90)

NGC 5929 is a type 2 Seyfert galaxy and is weakly detected in H I absorption. This is consistent with high-resolution H I MERLIN observations of the galaxy where absorption is seen against the north-eastern radio lobe ~0.5 arcsec from the nucleus (Cole et al. 1998). We do not detect any H I emission associated with either member of the interacting pair. However, there have been two previous detections of H I emission using single-dish radio telescopes. Huchtmeier (1982) found an H I flux of $3.1 \pm 1.9\,\mathrm{Jy\,km\,s^{-1}}$ using the 100-m radio telescope at Effelsberg (HPBW ~9 arcmin). Richter & Huchtmeier (1991) found an H I flux of $4.1 \pm 0.7\,\mathrm{Jy\,km\,s^{-1}}$ using the Greenbank 300-foot telescope (HPBW ~10 arcmin). Since the galaxies have no nearby companions, the H I must be significantly extended and therefore not detected by our snapshot observation.

4.5 NGC 7714 (Arp 284)

Weedman et al. (1981) classified NGC 7714 as an archetypal starburst galaxy, and it is well studied via optical, ultraviolet and

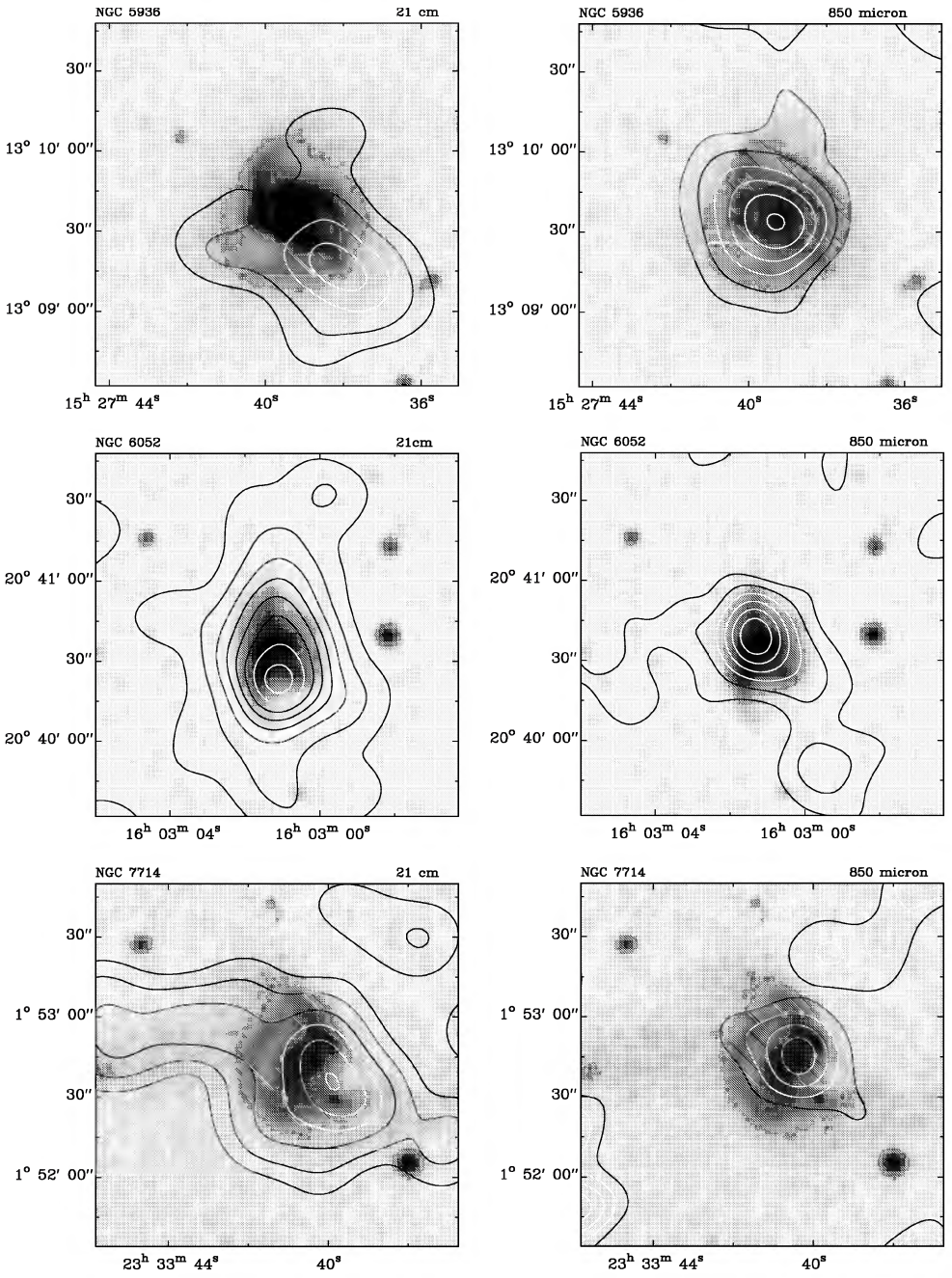

Figure 2 – *continued*

near-infrared spectroscopy (e.g. Garcia-Vargas et al. 1997; Gonzalez et al. 1999; O'Halloran et al. 2000; Kotilainen et al. 2001). The starburst is estimated to be 3–9 Myr old, and is known to contain Wolf–Rayet stars. The optical and H I maps clearly show a bridge of emission connecting the galaxy with its irregular companion NGC 7715, 1.9 arcmin away. Detailed VLA H I maps of the pair are presented by Smith & Wallin (1992) and Smith et al. (1997). The peak in the H I is offset from the centre of NGC 7714. This apparent offset is probably due to the absorption of gas against the bright continuum source. The 850-μm emission associated with this galaxy is essentially unresolved, but the peak in the emission is in reasonable agreement with the peak in the 1.4-GHz emission (Condon 1990).

5 DISCUSSION

5.1 H I emission/absorption

The H I distributions of the galaxies in this sample have a range of morphologies, although most fall into two categories: H I emission that is concentrated towards the centre of the galaxy (e.g. NGC 2990, NGC 3221); or a local H I minimum at the centre of the galaxy (e.g UGC 8739, NGC 5900, NGC 3110). However, several galaxies do not fall into either category: e.g. NGC 7714 and 3994/5, both of which are interacting. Galaxies with H II or LINER-type spectra appear to have the most disrupted discs; however, this is a tentative result as optical spectra do not exist for

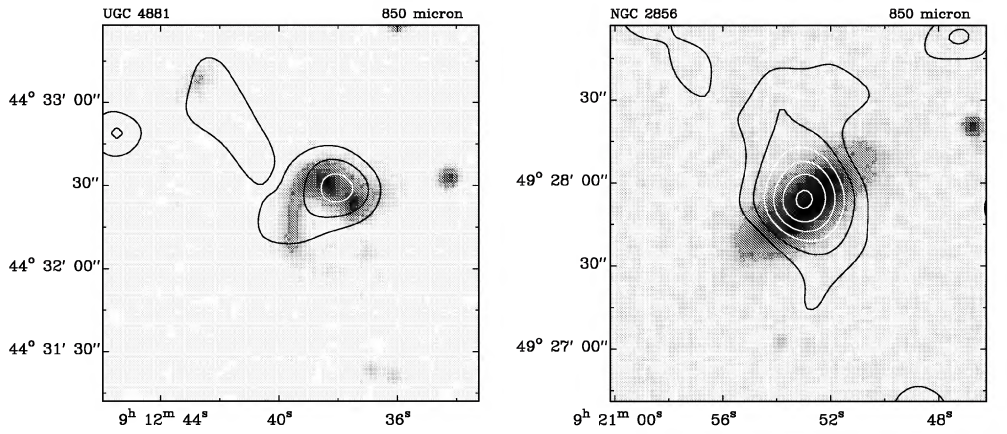

Figure 3. SCUBA 850-μm maps for those galaxies not detected in H I.

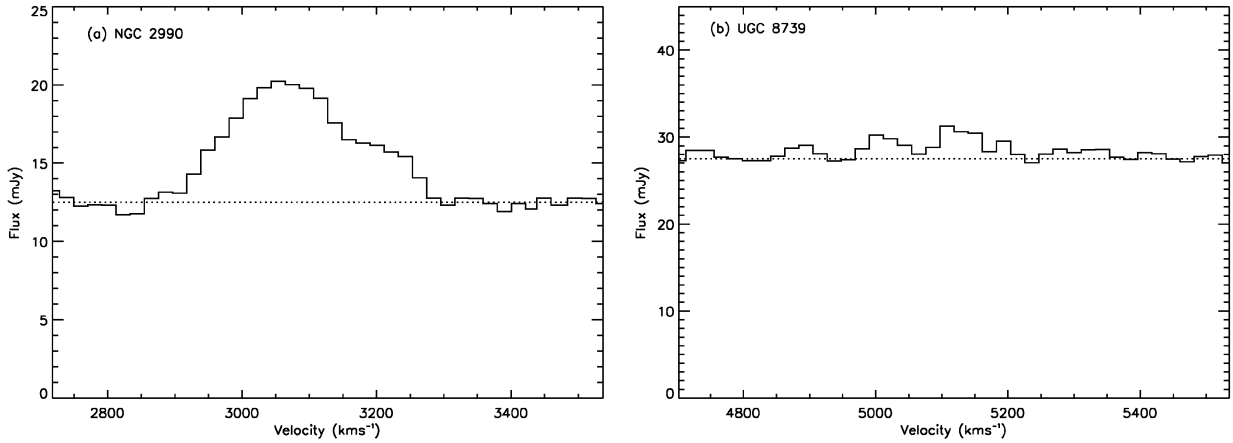

Figure 4. 21-cm spectra taken over a 25×25 arcsec^2 region centred on the galaxies (a) NGC 2990 and (b) UGC 8739. Note the difference in the strength of the continuum emission.

some of these galaxies. Two of the galaxies in the sample (both Seyferts) are detected in absorption against a bright nuclear continuum source. High-resolution (~6 arcsec) VLA maps have also shown H I absorption towards the nuclear regions of NGC 7714. The fact that this remains unresolved by our observations suggests that some of the other galaxies in our sample may suffer from some degree of absorption, and could explain the H I deficit observed in the central regions of some of these galaxies. However, unless the continuum emission contains a bright compact component behind a high concentration of gas, absorption may not be the primary cause of the deficit. Martin et al. (1991) observed a sample of 88 *IRAS*-bright galaxies and found a deficiency of H I which they attributed to a high rate of molecule formation and hence a high star formation rate. Using the results of Garwood, Helou & Dickey (1987) and Mirabel & Sanders (1988), they argued that H I absorption is negligible compared with the total amount of H I emission for each galaxy in their sample, and is only significant at a level $\log(L_{\rm fir}/{\rm L}_\odot) > 11$, becoming increasingly dominant with far-infrared luminosity. From Table 1 we see that three of the galaxies in our sample have $\log(L_{\rm fir}/{\rm L}_\odot) > 11$, one of which (NGC 3110) has the highest H_2-to-H I mass ratio out of the values listed. Overall, the H_2-to-H I mass ratio is 1.5–18 times that derived for our Galaxy.

In order to compare the H I and 850-μm emission, knowledge of H I absorption is crucial. We have attempted to estimate the effects of absorption in the following way. For each galaxy (except NGC 5929 and 4418), we produced a CLEANed data cube containing the 1.4-GHz continuum and the H I line emission, at a resolution of 25 arcsec. We then produced a spectrum of a 25×25 arcsec^2 area centred on the peak of the continuum emission. If the brightness temperature of the continuum source dominates over the H I then absorption is likely to occur. The brightness temperature, in the Rayleigh–Jeans limit, is given by

$$T_{\rm B} = \frac{\lambda^2 S}{2k\Omega f}, \qquad (1)$$

where S is the flux, Ω is the solid angle subtended by the beam (in units of steradians) and f is the filling factor. We measured the continuum flux and the peak H I flux from each spectrum. The filling factor for the continuum source was estimated by comparing the 25×25 arcsec^2 area with the size of the 1.4-GHz-emitting region given by Condon (1990). We assumed a filling factor of 1 for the H I emission. We found that the continuum emission becomes increasingly dominant over the H I emission as the brightness temperature of the continuum increases. There was also a tendancy for highly inclined galaxies to have the highest brightness temperatures. Fig. 4 shows spectra containing the 1.4-GHz continuum and line emission for (a) NGC 2990 (an example of a galaxy with centrally concentrated H I emission) and

(b) UGC 8739 (an example of a galaxy deficient in H I emission at the optical centre). Although these results are unsurprising, the fact that $T_B(1.4\,\mathrm{GHz})/T_B(\mathrm{H\,I})$ ranges from 1 to $\sim 10^4$ suggests that absorption is important in these galaxies. To estimate the size of the region that may be affected by absorption we looked at spectra away from the central regions of each galaxy. We found that beyond 30 arcsec $T_B(1.4\,\mathrm{GHz})/T_B(\mathrm{H\,I}) \ll 1$. Thus comparison of the 850-μm and H I emission in the central 30 arcsec of a galaxy should be treated with caution.

5.2 850-μm emission

Compared with the H I, the 850-μm emission appears less disturbed, and has a smooth distribution which is normally concentrated towards the optical centre of each galaxy.

Some of the galaxies, such as NGC 2785, appear to have 850-μm emission that extends to the periphery of the optical disc. However, none of the galaxies in this survey has an extended dust distribution comparable to that of NGC 7465 (Thomas et al. 2002) which stretches to at least $\sim 2R_{25}$. The two galaxies not detected in H I (see Fig. 3) do not appear to have significantly different 850-μm distributions from those that were detected in H I.

We have compared the 850-μm emission with the 1.4-GHz maps of Condon (1990). We find that there is a good agreement in the position of the 1.4-GHz and 850-μm peaks. At larger radii the distribution of 850-μm and 1.4-GHz emission is not always correlated. A more detailed analysis will be presented in subsequent papers.

5.3 Comparison between 850-μm and H I emission

The apparent absence of H I emission in the central regions of some of the galaxies makes it difficult to discern whether H I is a good predictor of 850-μm emission. If absorption is the primary cause of this deficit, then there may be a correlation between the H I and 850-μm emission. Comparison of the H I with molecular line observations would help to resolve this issue. At larger radii, there is evidence of a correlation between the H I and 850-μm emission in some of the galaxies. For example, note the similar morphology of the H I and 850-μm emission at the periphery of the optical disc of NGC 2785. Clearly, deeper SCUBA and VLA observations are required to ascertain the full extent of the 850-μm and H I emission at large radii. Although the H I emission is proportional to atomic gas mass, the 850-μm emission is a function of dust mass, dust temperature and grain properties. Thus a relative lack of 850-μm emission compared with the H I emission does not necessarily mean that the atomic gas and dust are not correlated. The distribution of the gas and dust masses will be the subject of future papers.

ACKNOWLEDGMENTS

We thank the referee for helpful criticism of the first version of this paper. We thank all of the support staff at the JCMT as well as any observers who took data on our behalf. The JCMT is operated by the Joint Astronomy Centre on behalf of the UK Particle Physics Research Council, the Netherlands Organization for Scientific Research and the Canadian National Research Council. The VLA is operated by the National Radio Astronomy Observatory for Associated Universities Inc., under a cooperative agreement with the National Science Foundation. The NASA/IPAC Extragalactic Database (NED) is operated by the Jet Propulsion Laboratory, California Institute of Technology, under contract with the National Aeronautics and Space Administration. The Digitized Palomar Sky Survey was funded by the National Geographic Society and produced by the Space Telescope Science Institute from plates taken from the Oschin Schmidt Telescope. This is operated jointly by the California Institute of Technology and the Palomar Observatory. HCT thanks PPARC for a research studentship.

REFERENCES

Alton P. B., Bianchi S., Rand R. J., Xilouris E. M., Davies J. I., Trewhella M., 1998, ApJ, 507, L125
Alton P. B., Xilouris E. M., Bianchi S., Davies J., Kylafis N., 2000, A&A, 356, 795
Alton P. B., Lequeux J., Bianchi S., Churches D., Davies J., Combes F., 2001, A&A, 366, 451
Arp H. C., 1966, ApJS, 14, 1
Artamonov B. P., Badan Y. Y., Gusev A. S., 2000, Astron. Rep., 44, 569
Baldwin J., Phillips M., Terlevich R., 1981, PASP, 93, 5
Bianchi S., Alton P. B., Davies J. I., Trewhella M., 1998, MNRAS, 298, L49
Bianchi S., Davies J. I., Alton P. B., Gerin M., Casoli F., 2000, A&A, 353, L13
Boulanger F., Abergel A., Bernard J. P., Burton W. B., Désert F. X., Hartmann D., Lagache G., Puget J. L., 1996, A&A, 312, 256
Casoli F., Dickey J., Kazes I., Boselli A., Gavazzi G., Jore K., 1996, A&AS, 116, 193
Cole G. H. J., Pedlar A., Mundell C. G., Gallimore J. F., Holloway A. J., 1998, MNRAS, 301, 1998
Condon J. J., 1990, ApJS, 73, 359
Condon J. J., Frayer D. T., Broderick J. J., 1991, AJ, 101, 362
Davies J. I., Alton P., Trewhella M., Evans R., Bianchi S., 1999, MNRAS, 304, 495
Dunne L., Eales S. A., Ivison R., Alexander P., Clements D. L., 2000, MNRAS, 315, 115
Garcia-Vargas M. L., Gonzalez-Delgado R. M., Perez E., Alloin D., Diaz A., Terlevich E., 1997, ApJ, 478, 112
Garwood R. W., Helou G., Dickey J. M., 1987, ApJ, 322, 88
Giovanelli R., Haynes M. P., 1988, in Verschur G. L., Kellermann K. I., eds, Galactic and Extragalactic Astronomy. Springer-Verlag, Berlin, p. 522
Gonzalez D., Roas M., Garcia-Vargas M. L., Goldader J., Leitherer C., Pasquali A., 1999, ApJ, 513, 707
Haas M., Klaas U., Coulson I., Thommes E., Xu C., 2000, A&A, 356, L83
Huchtmeier W. K., 1982, A&A, 110, 121
Kawara K., Taniguchi Y., Nakai N., Sofue Y., 1990, ApJ, 365, L1
Keel W. C., Kennicutt R. C., Hummel E., van Der Hulst J. M., 1985, AJ, 90, 708
Kenney J. D. P., Young J. S., 1989, ApJ, 344, 171
Kotilainen J. K., Reunanen J., Laine S., Ryder S. D., 2001, A&A, 366, 439
Maiolino R., Ruiz M., Rieke G. H., Papadopoulus P., 1997, ApJ, 485, 552
Martin J. M., Bottinelli L., Dennefeld M., Gouguenheim L., 1991, A&A, 245, 393
Mirabel I. F., Sanders D. B., 1988, ApJ, 335, 104
O'Halloran B., Metcalfe L., Delaney M., McBreen B., Laureijs R., Leech K., Watson D., Hanlon L., 2000, A&A, 360, 871
Richter O.-G., Huchtmeier W. K., 1987, A&AS, 68, 427
Richter O.-G., Huchtmeier W. K., 1991, A&AS, 87, 425
Roche P. F., Chandler C. J., 1993, MNRAS, 265, 486
Roche P. F., Aitken D. K., Smith C. H., James S. D., 1986, MNRAS, 218, 19
Sanders D. B., Scoville N. Z., Soifer B. T., 1991, ApJ, 370, 158

Smith B. J., Wallin J. F., 1992, ApJ, 393, 544
Smith B. J., Struck C., Pogge R. W., 1997, ApJ, 483, 754
Sodroski T. J., Odegard N., Arendt R. G., Dwek E., Weiland J. L., Hauser M. G., Kelsall T., 1997, ApJ, 480, 173
Sofue Y., Wakamatsu K., Taniguchi Y., Nakai N., 1993, PASJ, 45, 43
Spoon H. W. W., Keane J. V., Tielens A. G. G. M., Lutz D., Moorwood A. F. M., 2001, A&A, 365, 353
Thomas H. C., Dunne L., Clemens M. S., Alexander P., Eales S. A., Green D. A., James A., 2002, MNRAS, accepted
Trewhella M., Davies J. I., Alton P. B., Bianchi S., Madore B. F., 2000, ApJ, 543, 153
van Gorkom J. H., Ekers R. D., 1988, in Perley R. A., Schwab F. R., Bridle A. H., eds, Synthesis Imaging in Radio Astronomy. NRAO, p. 341
Weedman D. W., Feldman F. R., Balzano V. A., Ramsey L. W., Sramek R. A., Wuu C.-C., 1981, ApJ, 248, 105
Whittet D. C. B., 1992, Dust in the Galactic Environment. IoP Publishing, Bristol
Young J. S., Scoville N. Z., 1991, ARA&A, 29, 581

This paper has been typeset from a TEX/LATEX file prepared by the author.